



Public Health
England



NHS Breast Screening Programme Equipment Report

Technical Evaluation of IMS Giotto Class
digital mammography system in 2D mode

July 2019

Available from the National Co-ordinating Centre
for the Physics of Mammography (NCCPM)

About Public Health England

Public Health England exists to protect and improve the nation's health and wellbeing, and reduce health inequalities. We do this through world-leading science, knowledge and intelligence, advocacy, partnerships and the delivery of specialist public health services. We are an executive agency of the Department of Health and Social Care, and a distinct delivery organisation with operational autonomy. We provide government, local government, the NHS, Parliament, industry and the public with evidence-based professional, scientific and delivery expertise and support.

Public Health England
Wellington House
133-155 Waterloo Road
London SE1 8UG
Tel: 020 7654 8000

www.gov.uk/phe

Twitter: @PHE_uk

Facebook: www.facebook.com/PublicHealthEngland

www.gov.uk/phe/screening Twitter: @PHE_Screening Blog: phescreening.blog.gov.uk

Prepared by: N Tyler, K Young, JM Oduko, A Mackenzie.

For queries relating to this document, please contact: phe.screeninghelpdesk@nhs.net



© Crown copyright 2019

You may re-use this information (excluding logos) free of charge in any format or medium, under the terms of the Open Government Licence v3.0. To view this licence, visit [OG](http://www.og.gov.uk). Where we have identified any third party copyright information you will need to obtain permission from the copyright holders concerned.

Published June 2019

PHE publications

gateway number: GW-524

PHE supports the UN

Sustainable Development Goals



Contents

About PHE Screening	4
Executive summary	4
1. Introduction	5
1.1 Testing procedures and performance standards for digital mammography	5
1.2 Objectives	5
2. Methods	6
2.1 System tested	6
2.2 Output and HVL	7
2.3 Detector response	7
2.4 Dose measurement	8
2.5 Contrast-to-noise ratio	8
2.6 AEC performance for local dense areas	10
2.7 Noise analysis	11
2.8 Image quality measurements	12
2.9 Physical measurements of the detector performance	14
2.10 Other tests	14
3. Results	15
3.1 Output and HVL	15
3.2 Detector response	15
3.3 AEC performance	16
3.4 Noise measurements	20
3.5 Image quality measurements	22
3.6 Comparison with other systems	25
3.7 Detector performance	28
3.8 Other tests	30
4. Discussion	31
5. Conclusions	33
References	34

About PHE Screening

Screening identifies apparently healthy people who may be at increased risk of a disease or condition, enabling earlier treatment or informed decisions. National population screening programmes are implemented in the NHS on the advice of the UK National Screening Committee (UK NSC), which makes independent, evidence-based recommendations to ministers in the 4 UK countries. PHE advises the government and the NHS so England has safe, high quality screening programmes that reflect the best available evidence and the UK NSC recommendations. PHE also develops standards and provides specific services that help the local NHS implement and run screening services consistently across the country.

Executive summary

The purpose of the evaluation was to determine whether the IMS Giotto Class operating in 2D mode, meets the main standards in the NHS Breast Screening Programme (NHSBSP) and European protocols, and to provide performance data for comparison against other systems.

The mean glandular dose (MGD) was found to be well below the remedial level for all automatic exposure control (AEC) modes. For a 53mm equivalent standard breast, the MGD was 1.01mGy, compared with the remedial level of 2.5mGy. The image quality, measured by threshold gold thickness using the CDMAM test object, was at or better than the achievable level depending on the AEC mode.

The Giotto Class meets the requirements of the NHSBSP standards for digital mammography systems operating in 2D mode.

1. Introduction

1.1 Testing procedures and performance standards for digital mammography

This report is one of a series evaluating commercially available direct digital radiography (DR) systems for mammography on behalf of the NHSBSP. The testing methods and standards applied are mainly derived from NHSBSP Equipment Report 0604¹ which is referred to in this document as 'the NHSBSP protocol'. The standards for image quality and dose are the same as those provided in the European protocol,^{2,3} but the latter has been followed where it provides a more detailed standard, for example, for the automatic exposure control (AEC) system.

Some additional tests were carried out according to the UK recommendations for testing mammographic X-ray equipment as described in IPEM Report 89.⁴

1.2 Objectives

The aims of the evaluation were to:

- determine whether the IMS Giotto Class digital mammography system (operating in 2D mode) meets the main standards in the NHSBSP and European protocols
- provide performance data for comparison against other systems

2. Methods

2.1 System tested

The tests were conducted at the MIS Healthcare premises in London, on an IMS Giotto Class system as described in Table 1. The Giotto Class is shown in Figure 1.

Table 1. System description

Manufacturer	IMS
Model	Giotto Class
System serial number	1620032015
Target material	Tungsten (W)
Added filtration	50µm Silver (Ag)
Detector type	Amorphous selenium
Detector serial number	AP01-21353
Pixel size	85µm
Detector size	240mm x 300mm
Pixel array	2812 x 3580
Typical image sizes	19.7 MB
Pixel value offset	0
Source to detector distance	691mm
Source to table distance	672mm
Pre-exposure mAs	3-5m As depending on compressed breast thickness
AEC modes*	Standard, Dose, Contrast
Software version	Raffaello 4.4.0.0 – IMSProc 4.3.0.0

* At the time of testing these were described as Standard, Low and High

The 180mm x 240mm paddle was not available for use at the time of testing.

The Giotto Class can be tilted forwards or backwards, as indicated in Figure 1. It can also be tilted to the side, until the C-arm is horizontal, for performing biopsies (in conjunction with a prone table).



Figure 1. The IMS Giotto Class [credit: IMS]

2.2 Output and HVL

The output and half-value-layer (HVL) were measured as described in the NHSBSP protocol, at intervals of 3kV.

2.3 Detector response

The detector response was measured as described in the NHSBSP protocol, except that 3mm aluminium was used at the tubehead, instead of PMMA. The grid was removed and an ion chamber was positioned above the detector cover, 40mm from the chest wall edge (CWE). The incident air kerma was measured for a range of manually set mAs values at 29kV W/Ag anode/filter combination. The readings were corrected to the surface of the detector using the inverse square law. No correction was made for attenuation by the detector cover. A 10mm x 10mm region of interest (ROI) was positioned on the midline, 40mm from the CWE of each image. The average pixel value and the standard deviation of pixel values within the ROI were measured. The relationship between average pixel values and the incident air kerma to the detector was determined.

2.4 Dose measurement

Doses were measured using the X-ray set's AEC in the different modes to expose different thicknesses of PMMA. Each PMMA block had an area of 180mm x 240mm. Spacers were used to adjust the paddle height to be equal to the equivalent breast thickness, as shown in Table 3. The exposure factors were noted and mean glandular doses (MGDs) were calculated for equivalent breast thicknesses.

An aluminium square, 10mm x 10mm and 0.2mm thick, was used with the PMMA during these exposures, so that the images produced could be used for the calculation of the contrast-to-noise ratio (CNR), described in Section 2.5. The aluminium square was placed between 2, 10mm thick slabs of 180mm x 240mm PMMA, on the midline, with its centre 60mm from the CWE. Additional layers of PMMA were placed on top to vary the total thickness.

2.5 Contrast-to-noise ratio

Unprocessed images acquired during the dose measurement were analysed to obtain the CNRs. Thirty six small square ROIs (approximately 2.5mm x 2.5mm) were used to determine the average signal and the standard deviation in the signal within the image of the aluminium square (4 ROIs) and the surrounding background (32 ROIs), as shown in Figure 2. Small ROIs are used to minimise distortions due to the heel effect and other causes of non-uniformity.⁵ The CNR was calculated for each image, as defined in the NHSBSP and European Protocols.

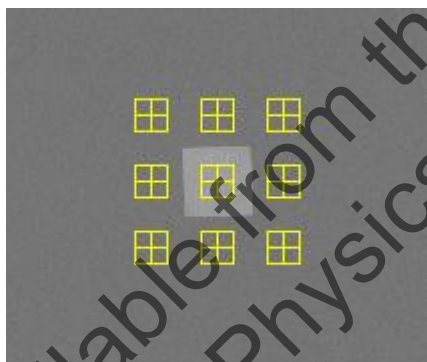


Figure 2. Location and size of ROI used to determine the CNR

To apply the standards in the European protocol, it is necessary to relate the image quality measured using the CDMAM (Section 2.8) for an equivalent breast thickness of 60mm, to that for other breast thicknesses. The European protocol² gives the relationship between threshold contrast and CNR measurements, enabling the calculation of a target CNR value for a particular level of image quality. This can be compared to CNR measurements made at other breast thicknesses. Contrast for a particular gold thickness is calculated using Equation 1, and target CNR is calculated using Equation 2,

$$\text{Contrast} = 1 - e^{-\mu t} \tag{Equation 1}$$

where μ is the effective attenuation coefficient for gold, and t is the gold thickness.

$$\text{CNR}_{\text{target}} = \frac{\text{CNR}_{\text{measured}} \times \text{TC}_{\text{measured}}}{\text{TC}_{\text{target}}} \tag{Equation 2}$$

Where $\text{CNR}_{\text{measured}}$ is the CNR for a 60mm equivalent breast, $\text{TC}_{\text{measured}}$ is the threshold contrast calculated using the threshold gold thickness for a 0.1mm diameter detail, (measured using the CDMAM at the same dose as used for $\text{CNR}_{\text{measured}}$), and $\text{TC}_{\text{target}}$ is the calculated threshold contrast corresponding to the threshold gold thickness required to meet either the minimum acceptable or achievable level of image quality as defined in the UK standard.

The threshold gold thickness for the 0.1mm diameter detail is used here because it is generally regarded as the most critical of the detail diameters for which performance standards are set.

The effective attenuation coefficient for gold used in Equation 1 depends on the beam quality used for the exposure, and the value used is in Table 2. This value was calculated with 3mm PMMA representing the compression paddle, using spectra from Boone et al.⁶ and attenuation coefficients for materials in the test objects (aluminium, gold, PMMA) from Berger et al.⁷

The European protocol also defines a limiting value for CNR, which is calculated as a percentage of the threshold contrast for minimum acceptable image quality for each thickness. This limiting value varies with thickness, as shown in Table 3.

Table 2. Effective attenuation coefficients for gold contrast details in the CDMAM

kV	Target/filter	Effective attenuation coefficient (μm^{-1})
31	W/Ag	0.104

Table 3. Limiting values for relative CNR

Thickness of PMMA (mm)	Equivalent breast thickness (mm)	Limiting values for relative CNR (%) in European protocol
20	21	> 115
30	32	> 110
40	45	> 105
45	53	> 103
50	60	> 100
60	75	> 95
70	90	> 90

The target CNR values for minimum acceptable and achievable levels of image quality and European limiting values for CNR were calculated. These were compared with the measured CNR results for all breast thicknesses.

2.6 AEC performance for local dense areas

This test is described in the supplement to the fourth edition of the European protocol.³ To simulate local dense areas, images of a 30mm thick block of PMMA of size 180mm x 240mm, were acquired under AEC, using the Standard dose mode. Extra pieces of PMMA between 2 and 20mm thick and of size 20mm x 40mm were added to provide extra attenuation. The compression plate remained in position at a height of 40mm, as shown in Figure 3. The simulated dense area was positioned 50mm from the CWE of the breast support table.

In the simulated local dense area the mean pixel value and standard deviation for a 10mm x 10mm ROI were measured and the signal-to-noise ratios (SNRs) were calculated.

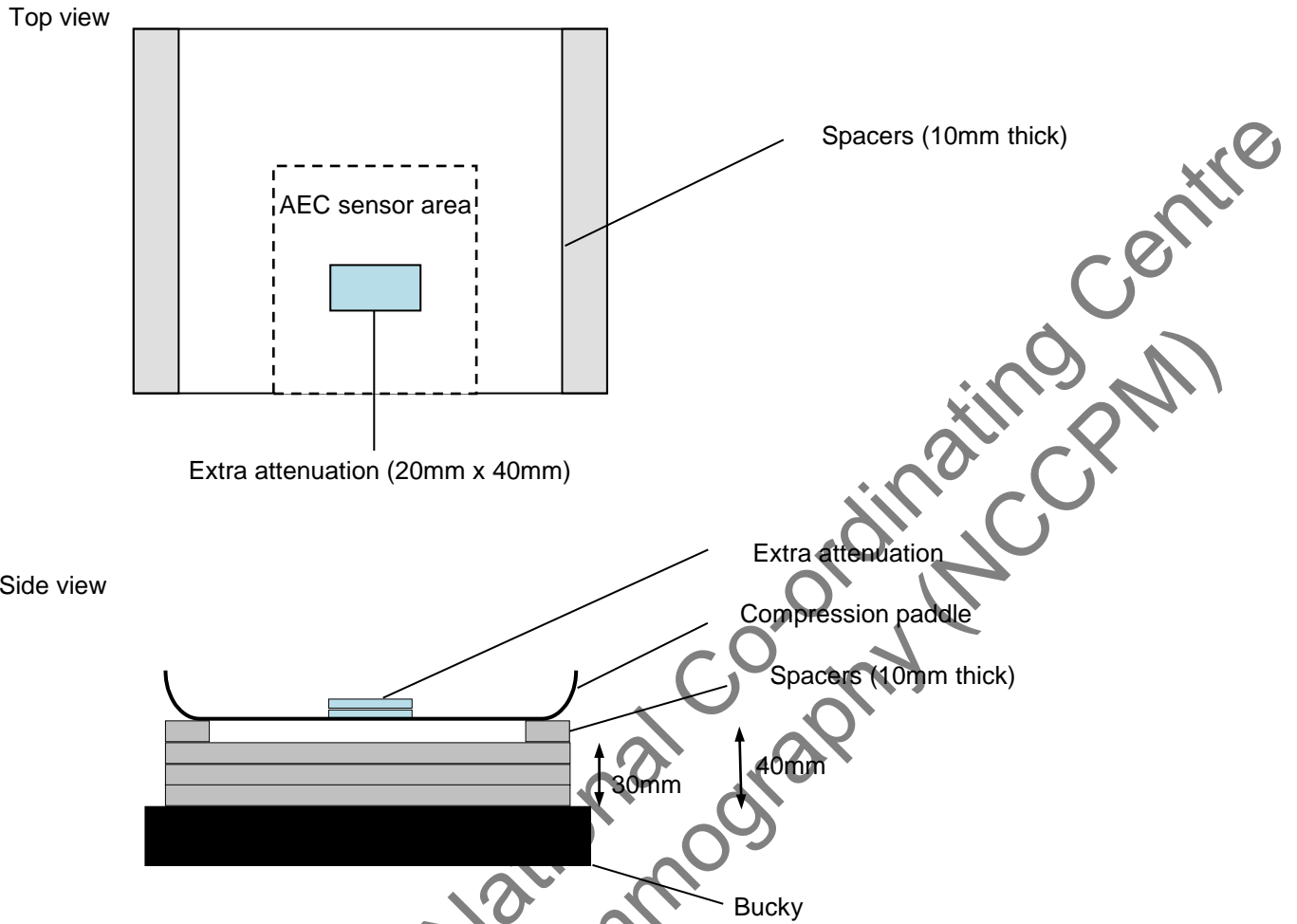


Figure 3. Setup to measure AEC performance for local dense areas

2.7 Noise analysis

The images acquired in the measurements of detector response, using 29kV W/Ag, were used to analyse the image noise. Small ROIs with an area of approximately 2.5mm x 2.5mm were placed on the midline, 60mm from the CWE. The average of the standard deviations of the pixel values in each of the ROIs for each image were used to investigate the relationship between the air kerma incident to the detector and the image noise. A power fit of standard deviation against incident air kerma was made. If electronic and structure noise are small then a square root relationship is expected. It was assumed that the noise in the image comprises 3 components: electronic noise, structural noise, and quantum noise. The relationship between them is shown in Equation 3:

$$\sigma_p = \sqrt{k_e^2 + k_q^2 p + k_s^2 p^2} \tag{Equation 3}$$

where σ_p is the standard deviation in pixel values within an ROI with a uniform exposure and a mean pixel value p , and k_e , k_q , and k_s are the coefficients determining the amount

of electronic, quantum, and structural noise in a pixel with a value p . This method of analysis has been described previously.⁸ For simplicity, the noise is generally presented here as relative noise defined as in Equation 4.

$$\text{Relative noise} = \frac{\sigma_p}{p} \quad (\text{Equation 4})$$

The variation in relative noise with mean pixel value was evaluated and fitted using Equation 3, and non-linear regression used to determine the best fit for the constants and their asymptotic confidence limits (using Graphpad Prism version 7.00 for Windows, Graphpad software, San Diego, California, USA, www.graphpad.com). This established whether the experimental measurements of the noise fitted this equation, and the relative proportions of the different noise components. The relationship between noise and pixel values has been found empirically to be approximated by a simple power relationship as shown in Equation 5, where k_t is a constant.

$$\frac{\sigma_p}{p} = k_t p^{-n} \quad (\text{Equation 5})$$

If the noise were purely quantum noise the value of n would be 0.5. However, the presence of electronic and structural noise means that n can be slightly higher or lower than 0.5. For graphical presentation in this report pixel values were converted to incident air kerma at the detector using the detector response data described in section 2.3.

The variance in pixel values within a ROI is defined as the standard deviation squared. The total variance against incident air kerma at the detector was fitted using Equation 3. Non-linear regression was used to determine the best fit for the constants and their asymptotic confidence limits, using the Graphpad Prism software.

Using the calculated constants, the structural, electronic, and quantum components of the variance were estimated, assuming that each component was independently related to incident air kerma. The percentage of the total variance represented by each component was then calculated and plotted against incident air kerma at the detector.

2.8 Image quality measurements

Contrast detail measurements were made using a CDMAM phantom (serial number 1022, version 3.4, UMC St. Radboud, Nijmegen University, Netherlands). The phantom was positioned with a 20mm thickness of PMMA above and below, to give a total attenuation approximately equivalent to 50mm of PMMA or 60mm thickness of typical breast tissue. The exposure factors were chosen to match as closely as possible those selected by the AEC, at the standard dose setting, when imaging a 50mm thickness of PMMA. This procedure was repeated to obtain a representative sample of 16 images at this dose level. Further sets of 16 images of the test phantom were then obtained at other dose levels by manually selecting higher and lower mAs values with the same beam quality.

The CDMAM images were read and analysed automatically using Version 1.6 of CDCOM.^{9,10} and Version 2.1.0 of CDMAM Analysis (www.nccpm.org). The threshold gold thickness for a typical human observer was predicted using Equation 6.

$$TC_{\text{predicted}} = rTC_{\text{auto}} \tag{Equation 6}$$

Where $TC_{\text{predicted}}$ is the predicted threshold contrast for a typical observer, TC_{auto} is the threshold contrast measured using an automated procedure with CDMAM images. r is the average ratio between human and automatic threshold contrast determined experimentally with the values shown in Table 4.

The contrasts used in Equation 6 were calculated from gold thickness using the effective attenuation coefficient shown in Table 2.

Table 4. Values of r used to predict threshold contrast

Diameter of gold disc (mm)	Average ratio of human to automatically measured threshold contrast (r)
0.08	1.40
0.10	1.50
0.13	1.60
0.16	1.68
0.20	1.75
0.25	1.82
0.31	1.88
0.40	1.94
0.50	1.98
0.63	2.01
0.80	2.06
1.00	2.11

The predicted threshold gold thickness for each detail diameter in the range 0.1mm to 1.0mm was fitted with a curve for each dose level, using the relationship shown in Equation 7.

$$\text{Threshold gold thickness} = a + bx^{-1} + cx^{-2} + dx^{-3} \tag{Equation 7}$$

Where x is the detail diameter, and a , b , c and d are coefficients adjusted to obtain a least squares fit.

The confidence limits for the predicted threshold gold thicknesses have been previously determined by a sampling method using a large set of images. The threshold contrasts quoted in the tables of results are derived from the fitted curves, as this has been found to improve accuracy.

The expected relationship between threshold contrast and MGD is shown in Equation 8,

$$\text{Threshold contrast} = \lambda D^{-n} \quad (8)$$

where D is the MGD for a 60mm thick standard breast (equivalent to the test phantom configuration used for the image quality measurement), and λ is a constant to be fitted.

It is assumed that a similar equation applies when using threshold gold thickness instead of contrast. This equation was plotted with the experimental data for detail diameters of 0.1 and 0.25mm. The value of n resulting in the best fit to the experimental data was determined, and the doses required for target CNR values were calculated for data relating to these detail diameters.

The MGDs to reach the minimum and achievable image quality standards in the NHSBSP protocol were then estimated. The error in estimating these doses depends on the accuracy of the curve fitting procedure, and pooled data for several systems has been used to estimate 95% confidence limits of about 20%.

2.9 Physical measurements of the detector performance

The modulation transfer function (MTF), normalised noise power spectrum (NNPS) and the detective quantum efficiency (DQE) of the system were measured. The methods used were as close as possible to those described by the International Electrotechnical Commission (IEC).¹¹ The radiation quality used for the measurements was adjusted by placing a uniform 3mm thick aluminium filter at the tube housing. The beam quality used was 29kV W/Ag. The test device to measure the MTF comprised a 120mm x 60mm rectangle of stainless steel with polished straight edges, of thickness 0.8mm. This test device was placed directly on the breast support table, and the grid was removed by selecting 'grid out' at the operator console. The test device was positioned to measure the MTF in 2 directions, first almost perpendicular to the CWE and then almost parallel to it. A tenth order polynomial fit was applied to the results.

To measure the noise power spectrum the test device was removed and exposures made for a range of incident air kerma at the surface of the table. The DQE is presented as the average of measurements in the directions perpendicular and parallel to the CWE.

2.10 Other tests

Other tests were carried out to cover the range that would normally form part of a commissioning survey on new equipment. These included tests prescribed in IPEM Report 89⁴ for mammographic X-ray sets, as well as those in the UK NHSBSP protocol for digital mammographic systems.

3. Results

3.1 Output and HVL

The output and HVL measurements are shown in Table 5.

Table 5. Output and HVL

kV	Target/ filter	Output ($\mu\text{Gy/mAs}$ at 1m)	HVL (mm Al)
25	W/Ag	12.9	0.49
28	W/Ag	18.8	0.55
31	W/Ag	24.4	0.59
34	W/Ag	29.9	0.61

3.2 Detector response

The detector response is shown in Figure 4.

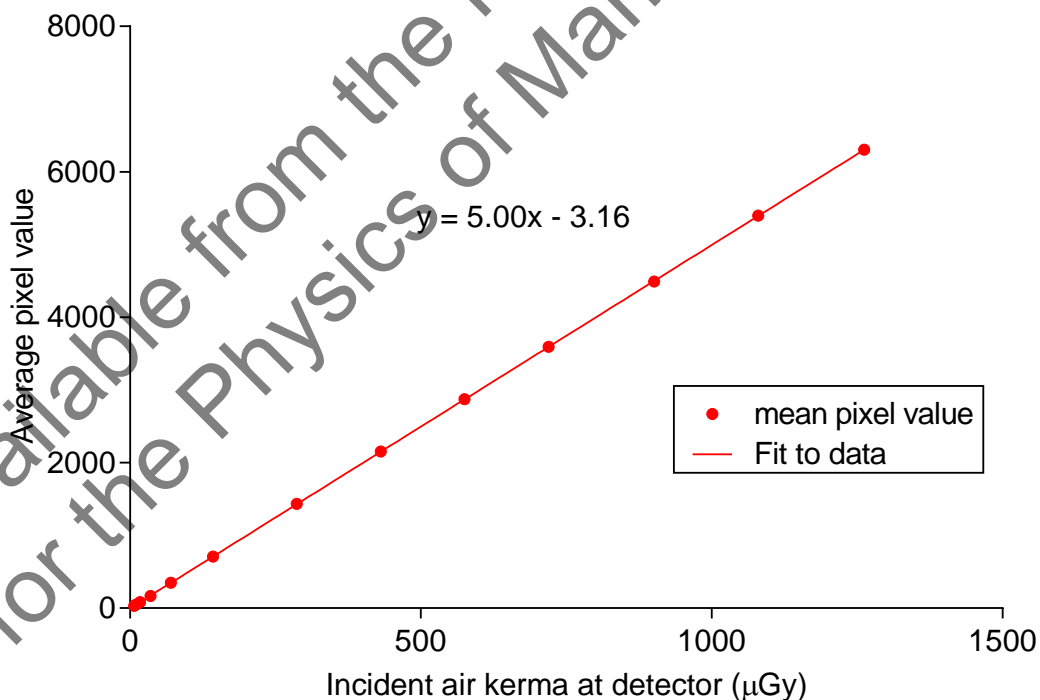


Figure 4. Detector response acquired at 29kV W/Ag anode/filter combination with 3mm Al at the tube port

3.3 AEC performance

3.3.1 Dose

The MGDs for breasts simulated with PMMA exposed using AEC Standard mode are shown in Tables 6 to 8 and Figure 5. The mAs values include the pre-exposure. The MGDs are calculated from the total mAs, including the pre-exposure.

Table 6. MGD for simulated breasts (Standard setting)

PMMA thickness (mm)	Equivalent breast thickness (mm)	kV	Target/ filter	mAs	MGD (mGy)	Remedial dose level (mGy)	Displayed dose (mGy)	Displayed % higher than MGD
20	21	25	W/Ag	35	0.52	1.0	0.5	-4.4%
30	32	26	W/Ag	47	0.66	1.5	0.6	-9.4%
40	45	28	W/Ag	57	0.90	2.0	0.9	0.0%
45	53	29	W/Ag	62	1.01	2.5	1.1	9.0%
50	60	31	W/Ag	61	1.16	3.0	1.2	3.6%
60	75	32	W/Ag	93	1.71	4.5	1.8	5.4%
70	90	34	W/Ag	118	2.20	6.5	2.4	9.0%

Table 7. MGD for simulated breasts (Dose setting)

PMMA thickness (mm)	Equivalent breast thickness (mm)	kV	Target/ filter	mAs	MGD (mGy)	Remedial dose level (mGy)	Displayed dose (mGy)	Displayed % higher than MGD
20	21	25	W/Ag	31	0.46	1.0	0.5	7.9%
30	32	26	W/Ag	41	0.58	1.5	0.6	3.9%
40	45	28	W/Ag	49	0.77	2.0	0.8	3.4%
45	53	30	W/Ag	47	0.85	2.5	0.9	5.9%
50	60	31	W/Ag	53	1.01	3.0	1.0	-0.7%
60	75	32	W/Ag	80	1.47	4.5	1.5	2.1%
70	90	34	W/Ag	101	1.88	6.5	2.0	6.2%

Table 8. MGD for simulated breasts (Contrast setting)

PMMA thickness (mm)	Equivalent breast thickness (mm)	kV	Target/ filter	mAs	MGD (mGy)	Remedial dose level (mGy)	Displayed dose (mGy)	Displayed % higher than MGD
20	21	25	W/Ag	45	0.67	1.0	0.7	4.1%
30	32	26	W/Ag	61	0.86	1.5	0.8	-6.9%
40	45	28	W/Ag	72	1.14	2.0	1.1	-3.3%
45	53	30	W/Ag	70	1.27	2.5	1.3	2.7%
50	60	31	W/Ag	77	1.46	3.0	1.5	2.5%
60	75	32	W/Ag	119	2.19	4.5	2.3	5.2%
70	90	34	W/Ag	151	2.82	6.5	3.1	10.1%

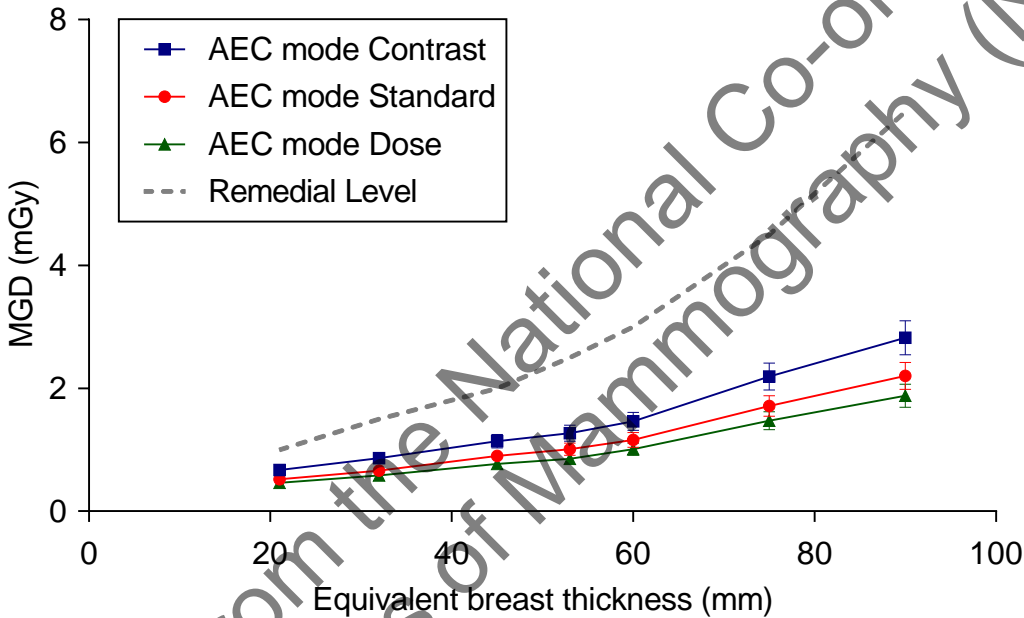


Figure 5. MGD for different thicknesses of simulated breasts at the 3 dose settings. (Error bars indicate 95% confidence limits.)

3.3.2 Contrast-to-Noise ratio

The results of the CNR measurements are shown in Table 9 and Figure 6. The following calculated values are also shown:

1. CNR to meet the minimum acceptable image quality standard at the 60mm breast thickness
2. CNR to meet the achievable image quality standard at the 60mm breast thickness
3. CNRs at each thickness to meet the limiting value in the European protocol

Table 9. CNR measurements for 3 AEC modes

PMMA (mm)	Equivalent breast thickness (mm)	Measured CNR			CNR for minimum acceptable IQ	CNR for achievable IQ	European limiting CNR value
		AEC mode: Standard	AEC mode: Dose	AEC mode: Contrast			
20	21	10.6	10.0	12.9	4.7	7.1	5.4
30	32	9.4	8.7	11.1	4.7	7.1	5.1
40	45	8.6	8.0	10.1	4.7	7.1	4.9
45	53	8.2	7.4	9.5	4.7	7.1	4.8
50	60	7.7	7.1	8.9	4.7	7.1	4.7
60	75	7.3	6.7	8.7	4.7	7.1	4.4
70	90	6.6	6.1	7.8	4.7	7.1	4.2

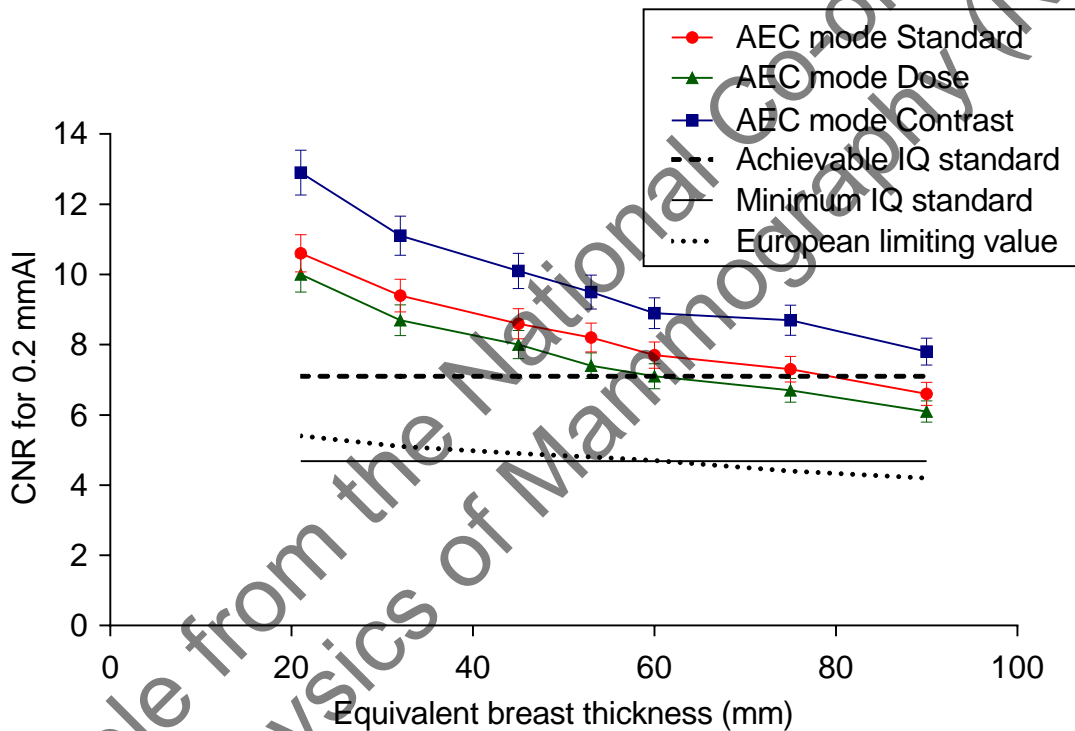


Figure 6. CNR measured using AEC at the 3 dose settings. (Error bars indicate 95% confidence limits.)

3.3.3 AEC performance for local dense areas

The test in the EUREF protocol² is based on an assumption that when the AEC adjusts for local dense areas, the SNR should remain constant with increasing thickness of extra PMMA. The results of this test are shown in Table 10 and Figure 7.

Figure 7 shows that the SNR varied by no more than 2.5% from the mean value while the local dense area was positioned on the midline, 50mm from the CWE of the breast support table. The tube load selected by the AEC was increased to achieve this constant SNR within the dense area.

Table 10. AEC performance for local dense areas

Total attenuation (mm PMMA)	kV	Target/filter	Tube load (mAs)	SNR	% SNR difference from mean SNR result
30	27	W/Ag	41	71.3	1.5
32	27	W/Ag	44	71.2	1.4
34	27	W/Ag	49	71.0	1.1
36	27	W/Ag	52	70.2	-0.04
38	27	W/Ag	57	68.7	-2.2
40	27	W/Ag	64	70.3	0.1
42	27	W/Ag	71	70.8	0.8
44	27	W/Ag	78	70.4	0.2
46	27	W/Ag	86	69.8	-0.6
48	27	W/Ag	92	68.7	-2.2

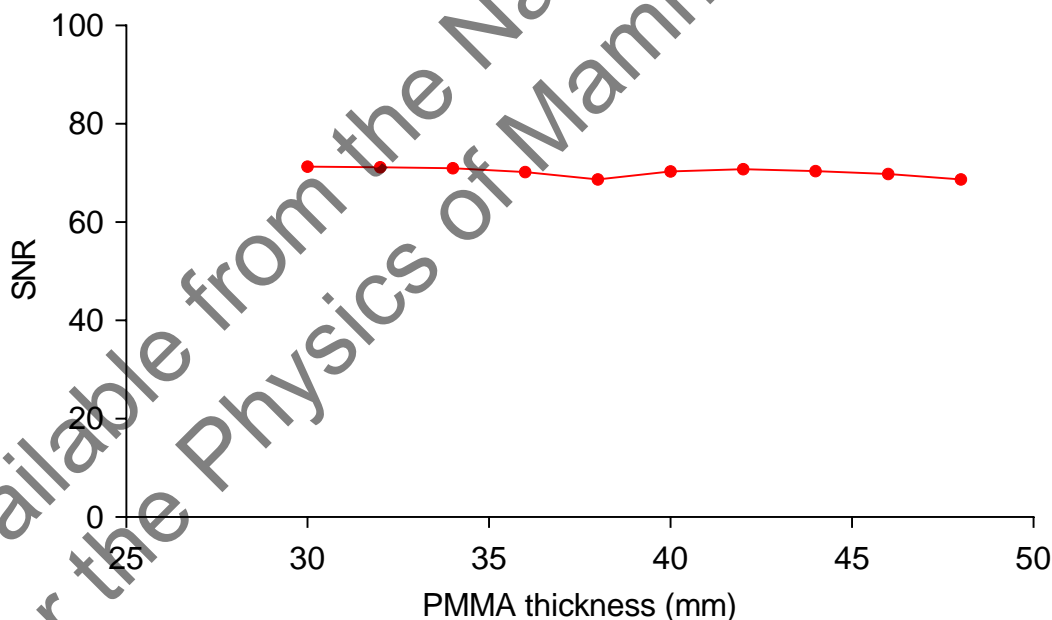


Figure 7. AEC performance for local dense areas

3.4 Noise measurements

The variation in noise with dose was analysed by plotting the standard deviation in pixel values against the incident air kerma to the detector, as shown in Figure 8. The fitted power curve has an index of 0.49, which is close to the expected value of 0.5 for quantum noise sources alone.

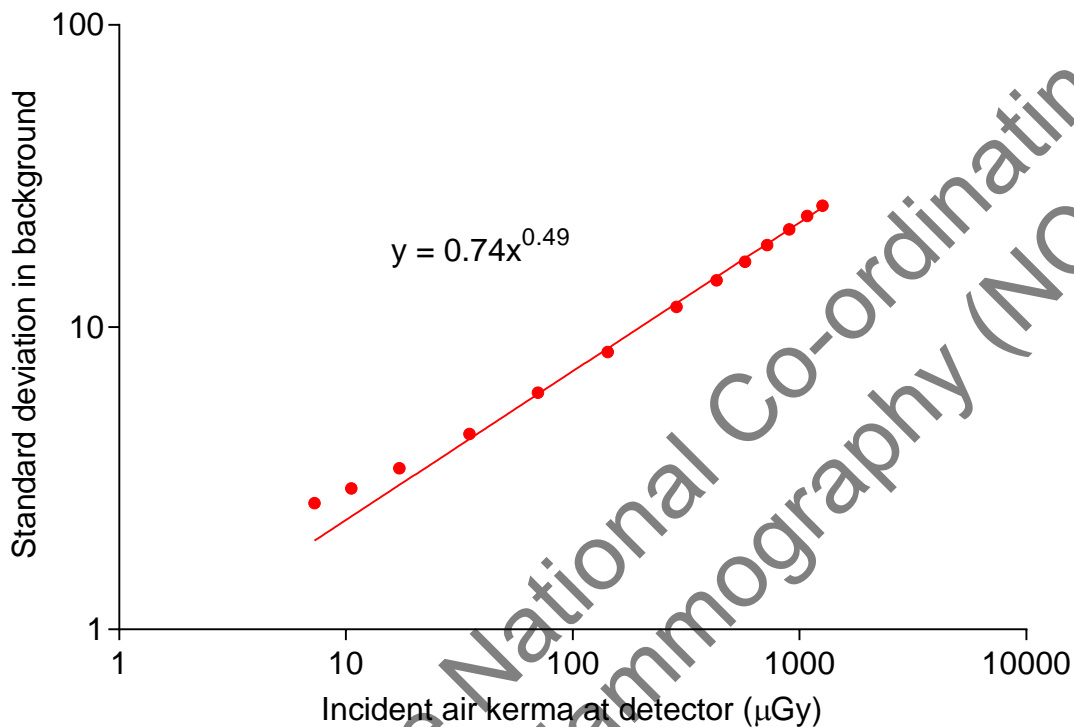


Figure 8. Standard deviation of linearized pixel values versus incident air kerma at detector

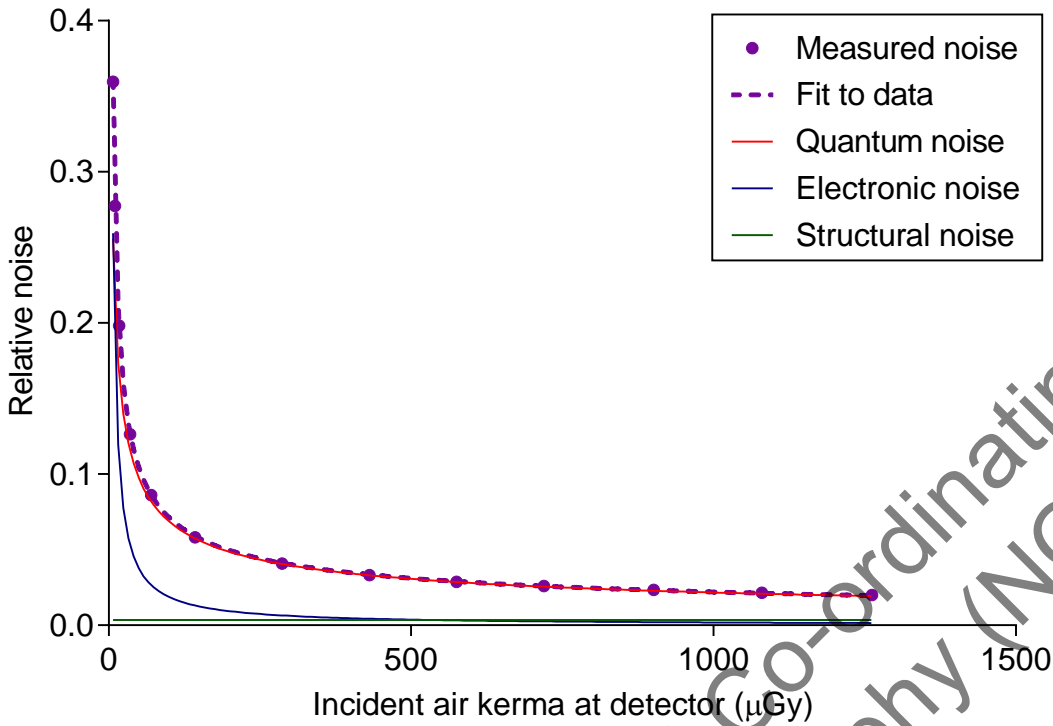


Figure 9. Relative noise and noise components

Figure 9 shows the relative noise at different incident air kerma. The estimated relative contributions of electronic, structural, and quantum noise are shown and the quadratic sum of these contributions fitted to the measured noise (using Equation 3).

Figure 10 shows the different amounts of variance due to each noise component. From this, the dose range over which the quantum component dominates can be seen.

Available from the National Co-ordinating Centre for the Physics of Mammography (NCCPM)

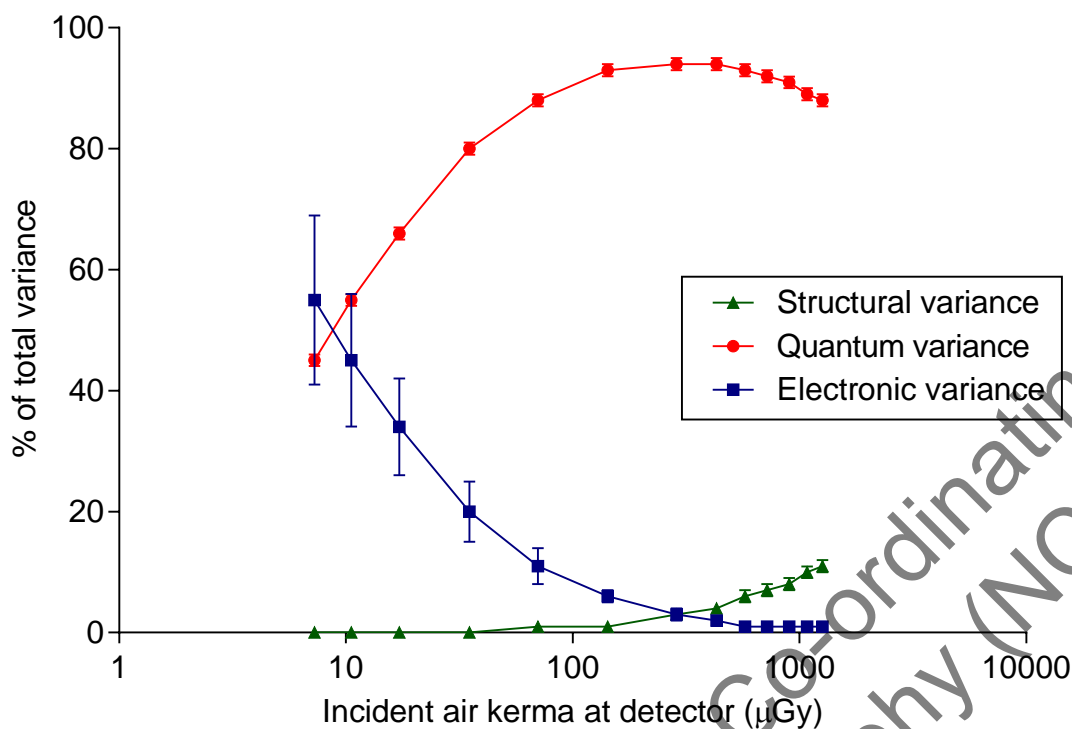


Figure 10. Noise components as a percentage of the total variance. (Error bars indicate 95% confidence limits.)

3.5 Image quality measurements

The exposure factors used for each set of 16 CDMAM images are shown in Table 11. The MGDs ranged from half to 3-times the dose of 1.16mGy, which was close to that selected for the equivalent breast of 60mm thick in Standard AEC mode.

Table 11. Images acquired for image quality measurement

kV	Target/filter	Tube loading (mAs)	Mean glandular dose to equivalent breasts 60mm thick (mGy)
31	W/Ag	30	0.57
31	W/Ag	45	0.85
31	W/Ag	61	1.16
31	W/Ag	90	1.71
31	W/Ag	180	3.42

The contrast detail curves (determined by automatic reading of the images) at the different dose levels are shown in Figure 11. The threshold gold thicknesses measured

for different detail diameters at the 5 selected dose levels are shown in Table 12. The NHSBSP minimum acceptable and achievable limits are also shown.

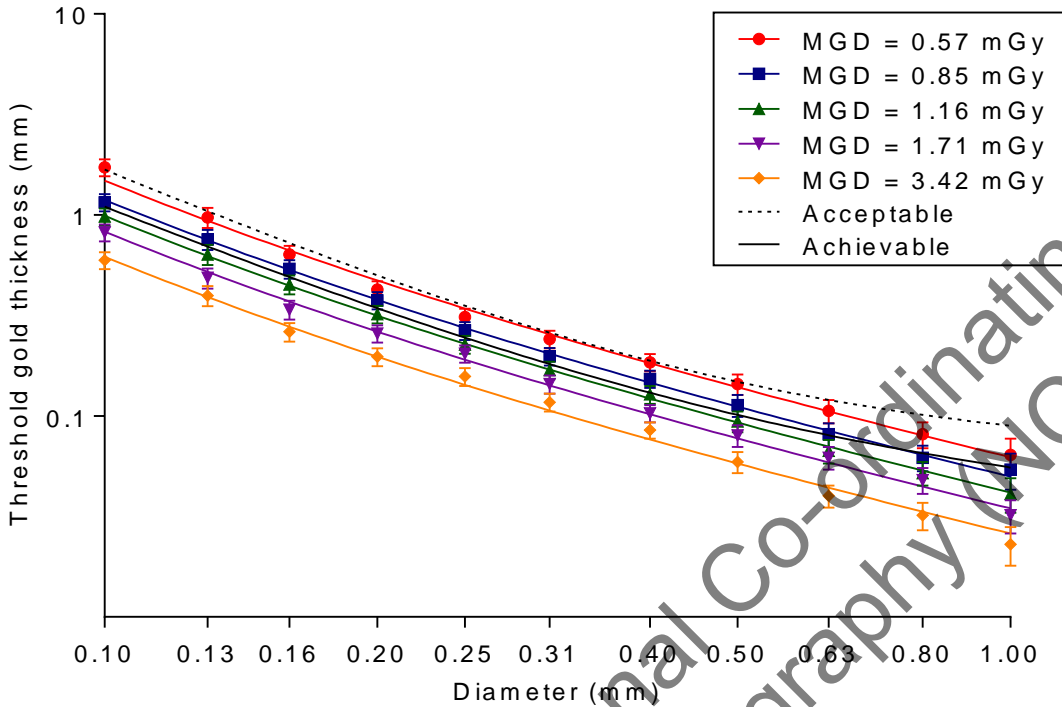


Figure 11. Threshold gold thickness detail detection curves for 5 doses at 31kV W/Ag. (Error bars indicate 95% confidence limits.)

Table 12. Average threshold gold thicknesses for different detail diameters for 5 doses using 31kV W/Ag, and automatically predicted data

Detail diameter (mm)	Threshold gold thickness (μm)						
	Acceptable value	Achievable value	MGD = 0.57mGy	MGD = 0.85mGy	MGD = 1.16mGy	MGD = 1.71mGy	MGD = 3.42mGy
0.1	1.680	1.100	1.72 ± 0.17	1.16 ± 0.11	0.98 ± 0.10	0.82 ± 0.08	0.60 ± 0.06
0.25	0.352	0.244	0.31 ± 0.03	0.27 ± 0.03	0.23 ± 0.02	0.20 ± 0.02	0.16 ± 0.02
0.5	0.150	0.103	0.14 ± 0.02	0.11 ± 0.01	$0.094 \pm$	$0.080 \pm$	$0.059 \pm$
1	0.091	0.056	$0.064 \pm$	$0.054 \pm$	$0.041 \pm$	$0.032 \pm$	$0.023 \pm$

The measured threshold gold thicknesses are plotted against the MGD for an equivalent breast for the 0.1mm and 0.25mm detail sizes in Figure 12.

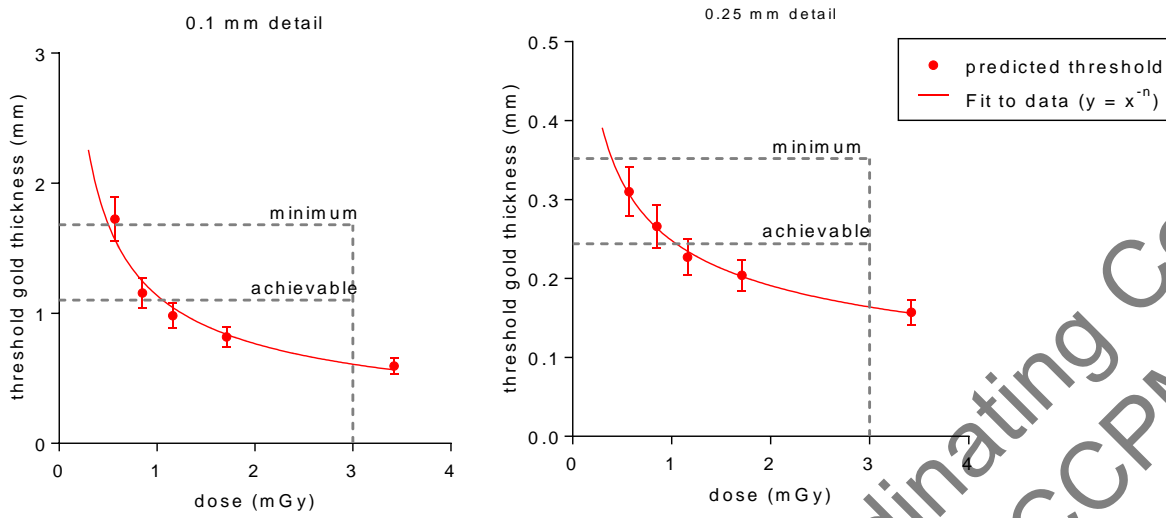


Figure 12. Threshold gold thickness at different doses. (Error bars indicate 95% confidence limits.)

Available from the National Coordinating Centre for the Physics of Mammography (NCCPM)

3.6 Comparison with other systems

The MGDs to reach the minimum and achievable image quality standards in the NHSBSP protocol have been estimated from the curves shown in Figure 12. These doses are shown against similar data for different models of digital mammography systems in Tables 13 and 14 and Figures 13 to 16. The data for these systems has been determined in the same way as described in this report and the results published previously.^{12,13,14,15,16,17,18} The data for film-screen represents an average value determined using a variety of film-screen systems in use prior to their discontinuation.

Table 13. The MGD for a 60mm equivalent breast for different systems to reach the minimum threshold gold thickness for 0.1mm and 0.25mm details

System	MGD (mGy) for 0.1mm	MGD (mGy) for 0.25mm
Fujifilm Innovality	0.61 ± 0.12	0.49 ± 0.10
GE Essential	0.49 ± 0.10	0.49 ± 0.10
Hologic Dimensions (v1.4.2)	0.34 ± 0.07	0.48 ± 0.10
Hologic Selenia (W)	0.71 ± 0.14	0.64 ± 0.13
IMS Giotto 3DL	0.93 ± 0.19	0.70 ± 0.14
IMS Giotto Class	0.50 ± 0.10	0.40 ± 0.08
Philips MicroDose L30 C120	0.67 ± 0.13	0.47 ± 0.09
Siemens Inspiration	0.76 ± 0.15	0.60 ± 0.12
Film-screen	1.30 ± 0.26	1.36 ± 0.27

Table 14. The MGD for a 60mm equivalent breast for different systems to reach the achievable threshold gold thickness for 0.1mm and 0.25mm details

System	MGD (mGy) for 0.1mm	MGD (mGy) for 0.25mm
Fujifilm Innovality	1.15 ± 0.23	1.02 ± 0.20
GE Essential	1.13 ± 0.13	1.03 ± 0.21
Hologic Dimensions (v1.4.2)	0.87 ± 0.17	1.10 ± 0.22
Hologic Selenia (W)	1.37 ± 0.27	1.48 ± 0.30
IMS Giotto 3DL	1.60 ± 0.32	1.41 ± 0.28
IMS Giotto Class	1.06 ± 0.21	1.05 ± 0.21
Philips MicroDose L30 C120	1.34 ± 0.27	1.06 ± 0.21
Siemens Inspiration	1.27 ± 0.25	1.16 ± 0.23
Film-screen	3.03 ± 0.61	2.83 ± 0.57

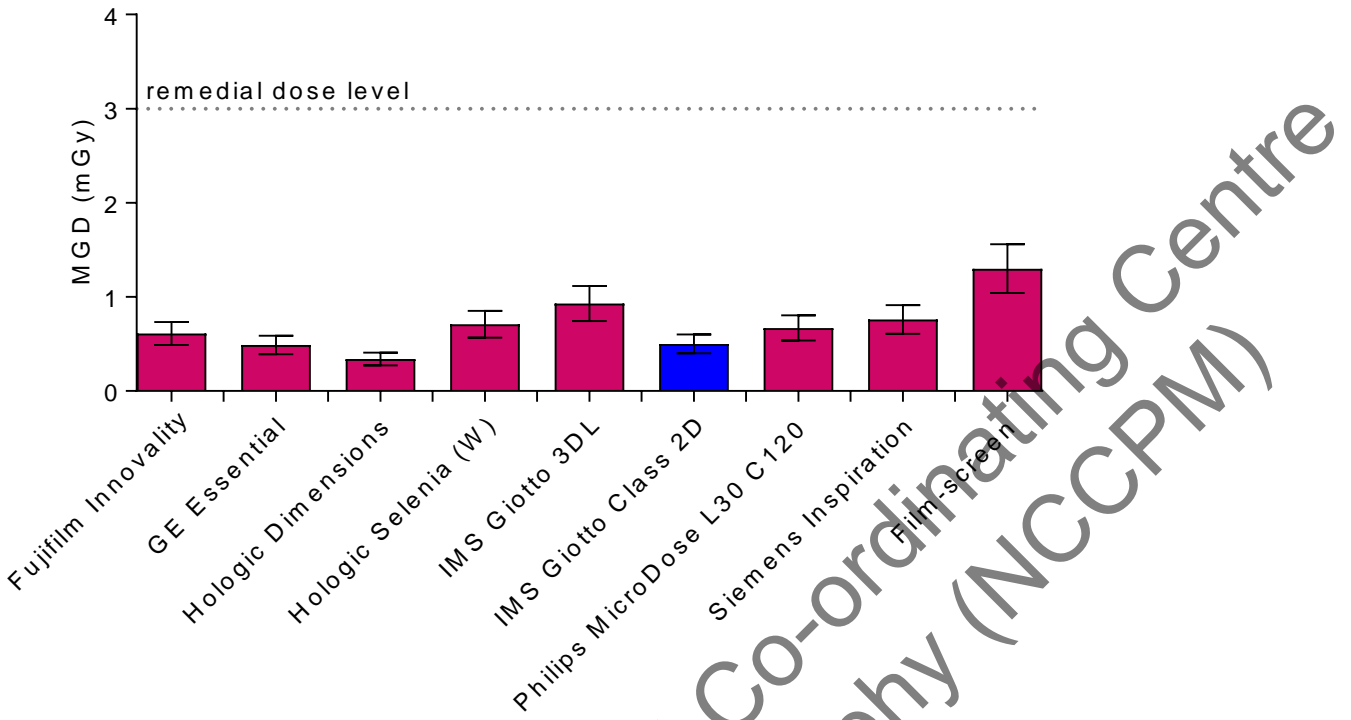


Figure 13. MGD for a 60mm equivalent breast to reach minimum acceptable image quality standard for 0.1mm detail. (Error bars indicate 95% confidence limits.)

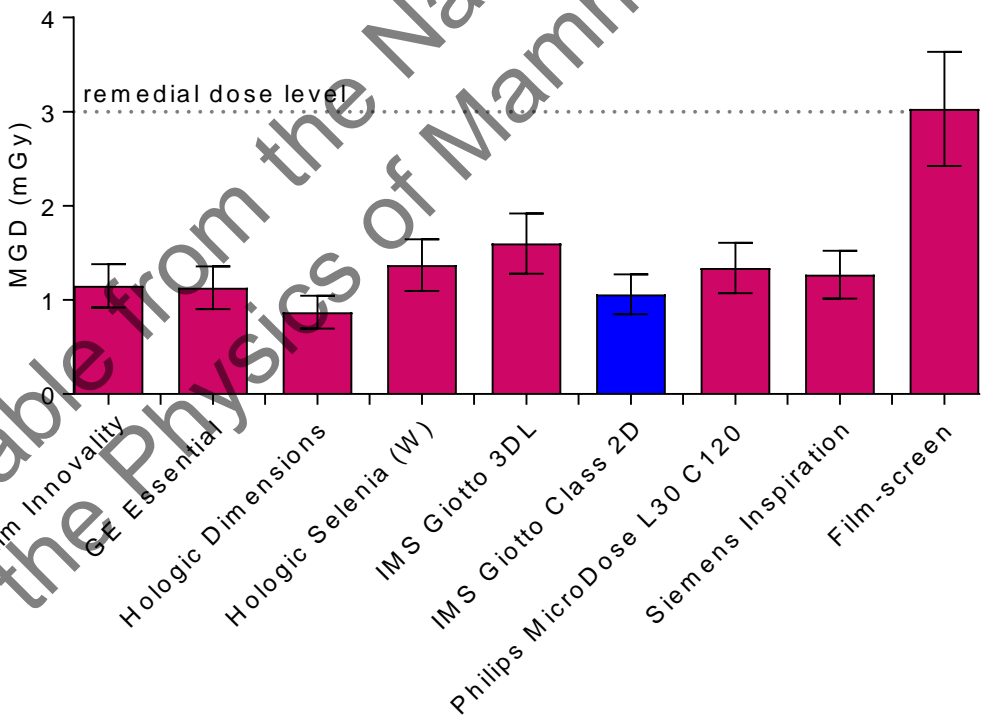


Figure 14. MGD for a 60mm equivalent breast to reach achievable image quality standard for 0.1mm detail. (Error bars indicate 95% confidence limits.)

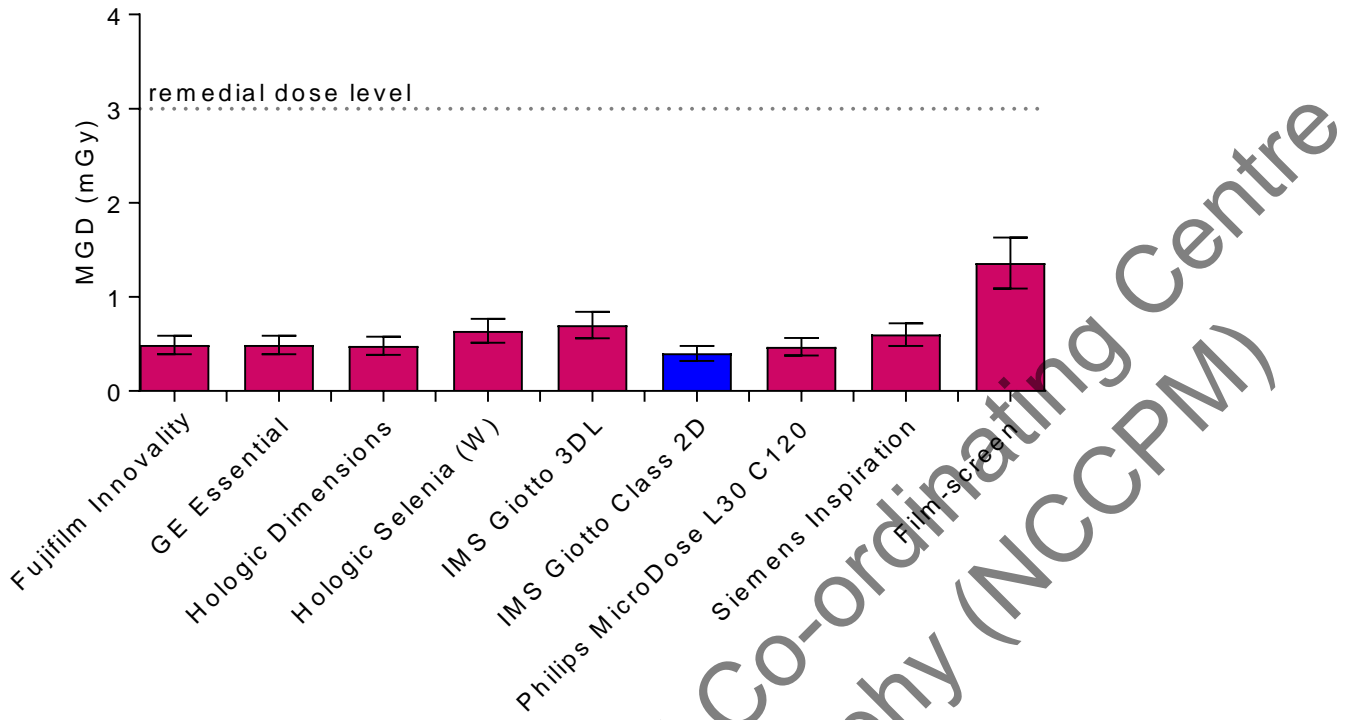


Figure 15. MGD for a 60mm equivalent breast to reach minimum acceptable image quality standard for 0.25mm detail. (Error bars indicate 95% confidence limits.)

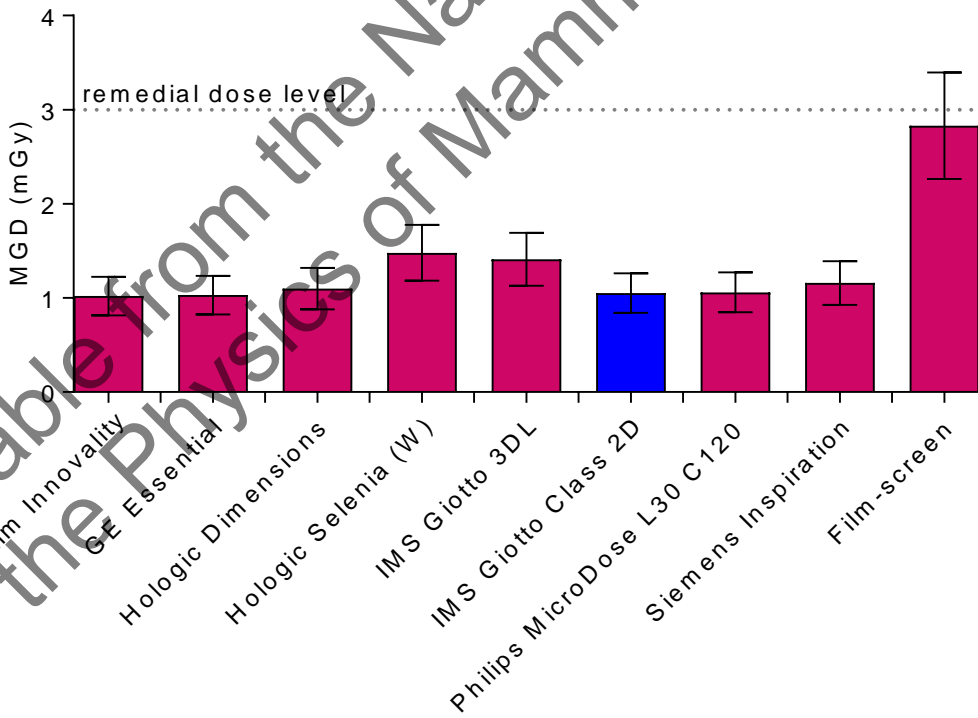


Figure 16. MGD for a 60mm equivalent breast to reach achievable image quality standard for 0.25mm detail. (Error bars indicate 95% confidence limits.)

3.7 Detector performance

The MTF is shown in Figure 17 for the 2 orthogonal directions. Figure 18 shows the NNPS curves for a range of air kerma incident to the detector.

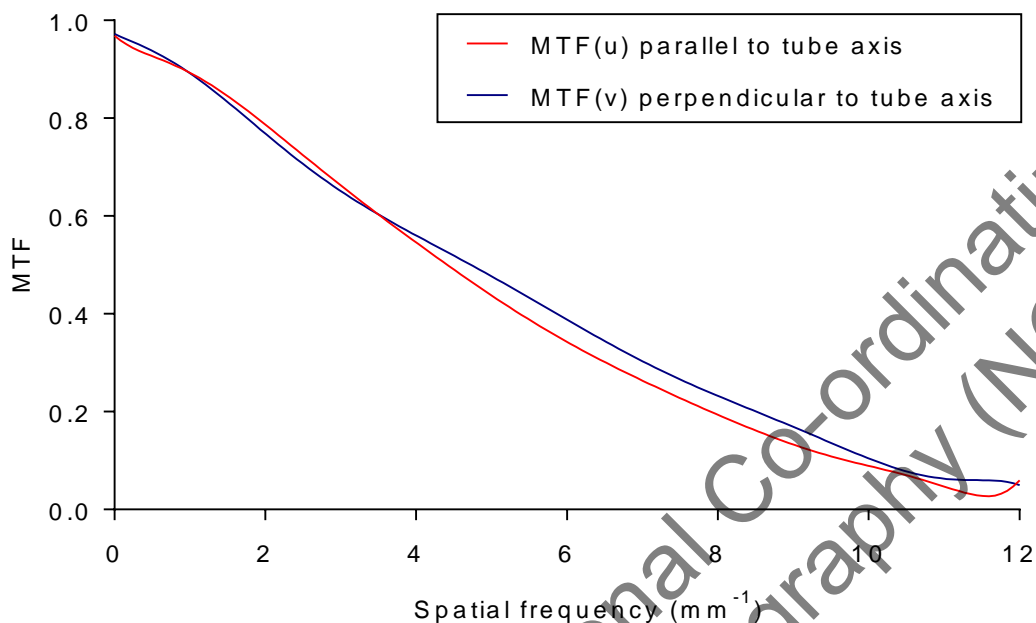


Figure 17. Pre-sampled MTF

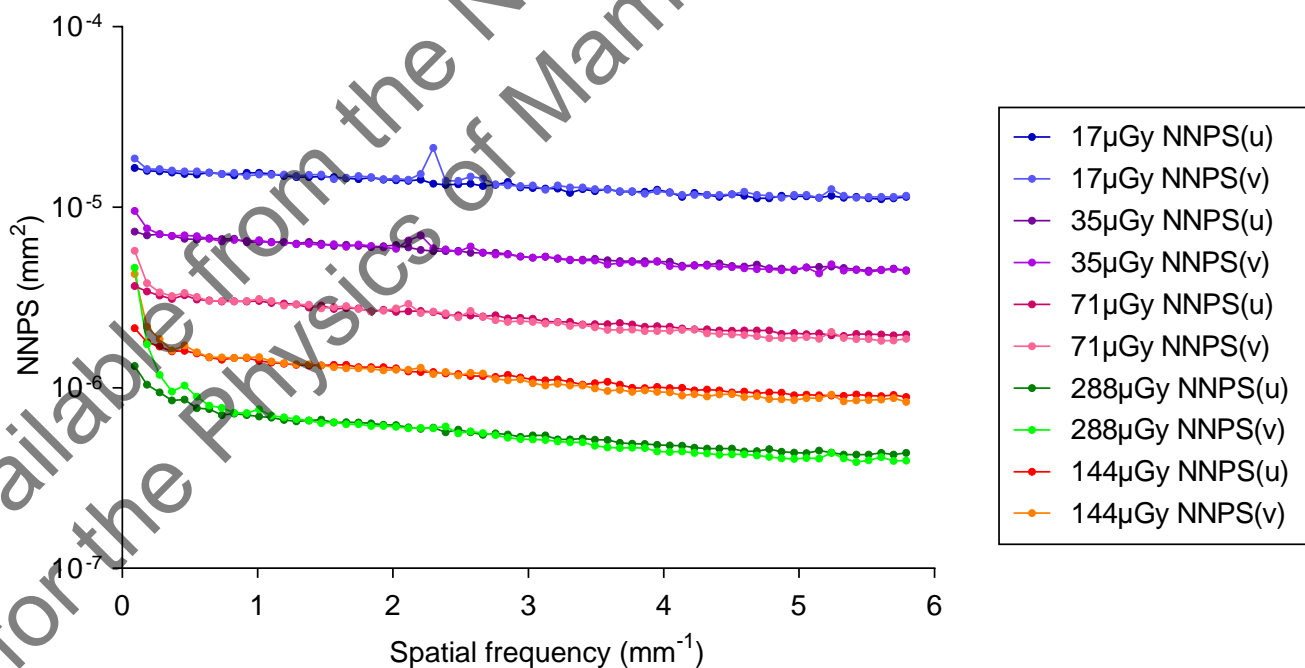


Figure 18. NNPS curves for a range of air kerma incident to the detector

Figure 19 shows the DQE averaged in the 2 orthogonal directions for a range of entrance air kerma. The MTF and DQE measurements were interpolated to show values at standard frequencies in Table 15.

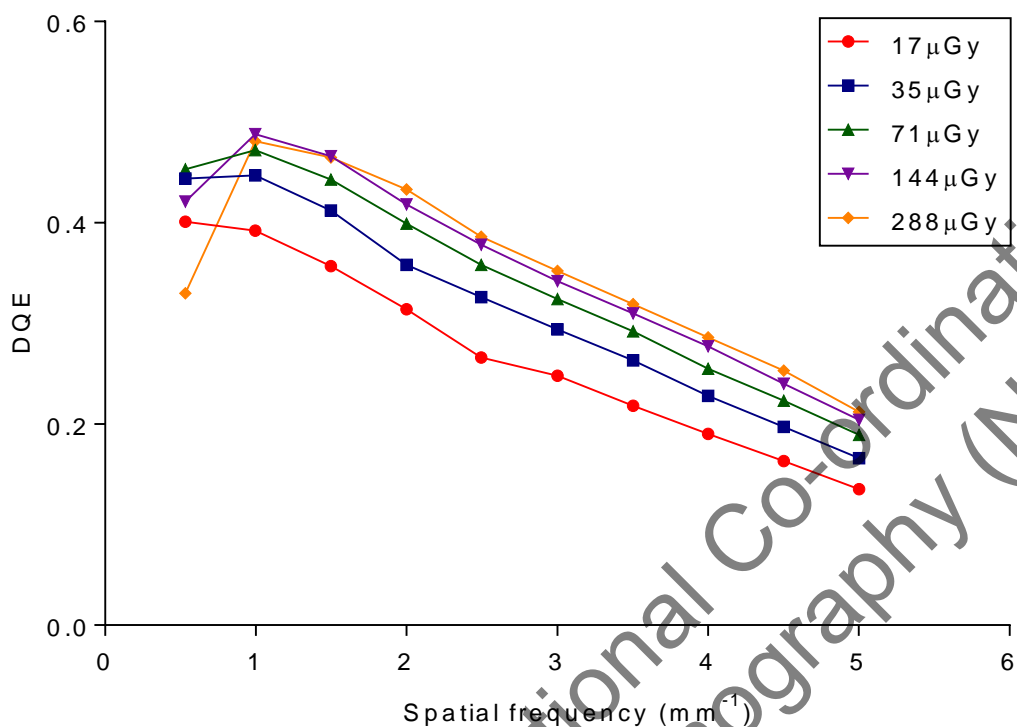


Figure 19. DQE averaged in both directions for a range of incident air kerma

Table 15. MTF and DQE measurements at standard frequencies (DQE at incident air kerma of 71μGy)

Frequency (mm ⁻¹)	MTF (u)	MTF (v)	DQE
0.0	1.00	1.00	-
0.5	0.92	0.94	0.45
1.0	0.89	0.89	0.47
1.5	0.85	0.83	0.44
2.0	0.79	0.77	0.40
2.5	0.73	0.71	0.36
3.0	0.66	0.65	0.32
3.5	0.60	0.60	0.29
4.0	0.55	0.56	0.26
4.5	0.49	0.52	0.22
5.0	0.44	0.48	0.19

3.8 Other tests

The results of all the other tests that were carried out were within acceptable limits as prescribed in the UK protocol and IPEM Report 89⁴.

3.8.1 Compression

The measured compressed breast thicknesses are compared with the displayed values in Table 16. There was 1 result outside of the IPEM Report 89⁴ remedial level of less than or equal to 5mm.

Table 16. Indicated compressed breast thickness

Actual thickness (mm)	Indicated thickness (mm)	Difference (mm)
20	26	6
30	34	4
40	43	3
50	53	3
60	65	5
70	74	4

3.8.2 Alignment

Initially the large penumbra of the X-ray field made it impossible to find a suitable position for the front collimator. After a modification to the design of the collimator by the manufacturer, the edge of the field was sharp and alignment was satisfactory.

3.8.3 Image retention

The image retention factor was 0.098, compared to the NHSBSP upper limit of 0.3.

3.8.4 AEC repeatability

There was less than 2% variation in mAs for a series of 5 repeat images, which compared favourably with the NHSBSP remedial level of 5%. The variation in SNR was also less than 2%.

3.8.5 Uniformity and artefacts

Uniformity measurements showed a variation in pixel values of less than 5% relative to the central area. The NHSBSP remedial level is 10%. There was a very faint 2mm pale band along the CWE.

4. Discussion

4.1 Dose and contrast-to-noise ratio

The detector response was found to be linear. This was as expected for the Giotto system.

MGDs measured using PMMA were well within the NHSBSP remedial dose levels for all equivalent breast thicknesses at all 3 AEC modes (Figure 5). The MGDs to a 53mm equivalent breast thickness were 0.85mGy, 1.01mGy and 1.27mGy respectively for the Dose, Standard and Contrast modes (Tables 6 to 8).

CNR measurements made with plain PMMA showed an overall decrease in CNR with increased thickness of PMMA for all 3 dose modes. Target CNR values of 4.7 and 7.1, for minimum acceptable and achievable image quality respectively, were calculated from the CNR and threshold gold thickness results.

In the Standard AEC mode, the CNRs exceeded the target for the achievable level of image quality for equivalent breast thicknesses of up to 75mm. For a 90mm equivalent breast thickness, the CNR was below the achievable level.

In the Dose AEC mode, the CNRs exceeded the target for the achievable level of image quality for equivalent breast thicknesses of up to 60mm. In the Contrast AEC mode, the CNRs exceeded the target for the achievable level of image quality for equivalent breast thicknesses of up to 90mm.

4.2 Local dense area

The local dense area test showed that the SNR was maintained to within 2.5% of the mean SNR value of additional thickness of PMMA up to 18mm (Table 10).

4.3 Noise analysis

Noise analysis showed that quantum noise dominates the noise at the AEC operating level (Figure 10). There are minimal contributions from structural noise. The electronic noise is dominant below 10 μ Gy.

4.4 Image quality

Threshold gold thicknesses for a range of detail diameters are shown in Figure 11. At an MGD of 1.16mGy (close to that selected for the equivalent thickness of PMMA in

Standard mode), the image quality was better than the achievable level for all contrast detail diameters.

The dose required for the Giotto Class to reach the achievable level of image quality was comparable to that measured for other direct digital mammography systems (Tables 13 and 14 and Figures 13 to 16).

4.5 Detector performance

The detector performance, as indicated by MTF, NNPS and DQE curves (Figures 17 to 19), was provided for reference and was within expected results.

4.6 Other tests

The miscellaneous results presented under the section 'Other tests' were satisfactory.

Available from the National Co-ordinating Centre
for the Physics of Mammography (NCCPM)

5. Conclusions

The IMS Giotto Class in 2D mode meets the minimum requirements of the NHSBSP standards for digital mammography systems when operating in the Dose, Standard or Contrast AEC modes.

The MGD is below the remedial level for all AEC modes. In standard mode, the MGD for a breast thickness of 53mm was 1.01mGy. The image quality, as measured by threshold gold thickness, is better than the achievable level.

In the Standard mode the image quality exceeds the minimum acceptable level for all equivalent breast thicknesses up to 90mm and exceeds the achievable level for equivalent breast thicknesses up to 75mm (60mm PMMA). Ideally, the achievable level of image quality should be met for all breast thicknesses. This could be achieved by using the Contrast AEC setting for breasts above 75mm thick.

Available from the National Co-ordinating Centre
for the Physics of Mammography (NCCPM)

References

1. Kulama E, Burch A, Castellano I et al. *Commissioning and routine testing of full field digital mammography systems* (NHSBSP Equipment Report 0604, Version 3). Sheffield: NHS Cancer Screening Programmes, 2009
2. van Engen R, Young KC, Bosmans H, et al. European protocol for the quality control of the physical and technical aspects of mammography screening. In *European guidelines for quality assurance in breast cancer screening and diagnosis*, Fourth Edition. Luxembourg: European Commission, 2006
3. van Engen R, Bosmans H, Dance D et al. Digital mammography update: European protocol for the quality control of the physical and technical aspects of mammography screening. In *European guidelines for quality assurance in breast cancer screening and diagnosis*, Fourth edition – Supplements. Luxembourg: European Commission, 2013
4. Moore AC, Dance DR, Evans DS et al. *The Commissioning and Routine Testing of Mammographic X-ray Systems*. York: Institute of Physics and Engineering in Medicine, Report 89, 2005
5. Alsager A, Young KC, Oduko JM. Impact of heel effect and ROI size on the determination of contrast-to-noise ratio for digital mammography systems. In *Proceedings of SPIE Medical Imaging*, Bellingham WA: SPIE Publications, 2008, 691341: 1-11
6. Boone JM, Fewell TR and Jennings RJ. Molybdenum, rhodium and tungsten anode spectral models using interpolating polynomials with application to mammography *Med. Phys.*, 1997, 24: 1863-1974
7. Berger MJ, Hubbell JH, Seltzer SM, Chang et al. XCOM: Photon Cross Section Database (version 1.3) <http://physics.nist.gov/xcom> (Gaithersburg, MD, National Institute of Standards and Technology), 2005
8. Young KC, Oduko JM, Bosmans H, Nijs K, Martinez L. Optimal beam quality selection in digital mammography. *Brit. J. Radiol.*, 2006, 79: 981-990
9. Young KC, Cook JH, Oduko JM. Automated and human determination of threshold contrast for digital mammography systems. In *Proceedings of the 8th International Workshop on Digital Mammography*, Berlin: Springer-Verlag, 2006, 4046: 266-272
10. Young KC, Alsager A, Oduko JM et al. Evaluation of software for reading images of the CDMAM test object to assess digital mammography systems. In *Proceedings of SPIE Medical Imaging*, Bellingham WA: SPIE Publications, 2008, 69131C: 1-11
11. IEC 62220-1-2, *Determination of the detective quantum efficiency – Detectors used in mammography*. International Electrotechnical Commission, 2007

12. Young KC, Oduko JM. *Technical evaluation of the Hologic Selenia full field digital mammography system with a tungsten tube* (NHSBSP Equipment Report 0801). Sheffield: NHS Cancer Screening Programmes, 2008
13. Young KC, Oduko JM, Gundogdu O and Asad M. *Technical evaluation of profile automatic exposure control software on GE Essential FFDM systems* (NHSBSP Equipment Report 0903). Sheffield: NHS Cancer Screening Programmes, 2009
14. Young KC, Oduko JM, Gundogdu, O, Alsager, A. *Technical evaluation of Siemens Mammomat Inspiration Full Field Digital Mammography System* (NHSBSP Equipment Report 0909). Sheffield: NHS Cancer Screening Programmes, 2009
15. Young KC, Oduko JM. *Technical evaluation of Hologic Selenia Dimensions 2-D Digital Breast Imaging System with software version 1.4.2* (NHSBSP Equipment Report 1201). Sheffield: NHS Cancer Screening Programmes, 2012
16. Strudley CJ, Young KC, Oduko JM. *Technical Evaluation of the IMS Giotto 3DL Digital Breast Imaging System* (NHSBSP Equipment Report 1301). Sheffield: NHS Cancer Screening Programmes, 2013
17. Oduko JM, Young KC. *Technical evaluation of Philips MicroDose L30 with AEC software version 8.3* (NHSBSP Equipment Report 1305). Sheffield: NHS Cancer Screening Programmes, 2013
18. Strudley CJ, Oduko JM, Young KC. *Technical evaluation of the Fujifilm AMULET Innovality Digital Breast Imaging System* (NHSBSP Equipment Report 1601). London, Public Health England, 2017

Available from the National Co-ordinating Centre
for the Physics of Mammography (NCCPM)